NANO LETTERS

Letter

pubs.acs.org/NanoLett

Nanocrystals of Cesium Lead Halide Perovskites ($CsPbX_3$, X = Cl, Br, and I): Novel Optoelectronic Materials Showing Bright Emission with Wide Color Gamut

Loredana Protesescu,[†,‡] Sergii Yakunin,[†,‡] Maryna I. Bodnarchuk,[†,‡] Franziska Krieg,[†,‡] Riccarda Caputo,[†] Christopher H. Hendon,[§] Ruo Xi Yang,[§] Aron Walsh,[§] and Maksym V. Kovalenko*[,†,‡]

[†]Institute of Inorganic Chemistry, Department of Chemistry and Applied Biosciences, ETH Zürich, Vladimir Prelog Weg 1, CH-8093 Zürich, Switzerland

[‡]Laboratory for Thin Films and Photovoltaics, Empa – Swiss Federal Laboratories for Materials Science and Technology, Überlandstrasse 129, CH-8600 Dübendorf, Switzerland

[§]Centre for Sustainable Chemical Technologies and Department of Chemistry, University of Bath, Bath BA2 7AY, United Kingdom

Supporting Information

ABSTRACT: Metal halides perovskites, such as hybrid organic–inorganic $CH_3NH_3PbI_3$, are newcomer optoelectronic materials that have attracted enormous attention as solution-deposited absorbing layers in solar cells with power conversion efficiencies reaching 20%. Herein we demonstrate a new avenue for halide perovskites by designing highly luminescent perovskite-based colloidal quantum dot materials. We have synthesized monodisperse colloidal nanocubes (4–15 nm edge lengths) of fully inorganic cesium lead halide perovskites ($CsPbX_3$, X = Cl, Br, and I or mixed halide systems Cl/Br and Br/I) using inexpensive commercial precursors. Through compositional modulations and quantum size-effects, the bandgap energies and emission spectra are readily tunable over the entire visible spectral region of 410–700 nm. The photoluminescence of $CsPbX_3$ nanocrystals is characterized by narrow emission line-widths of 12–42 nm, wide color gamut covering up to 140% of the NTSC color standard, high quantum yields of up to 90%, and radiative lifetimes in the range of 1–29 ns. The compelling combination of enhanced optical properties and chemical robustness makes $CsPbX_3$ nanocrystals appealing for optoelectronic applications, particularly for blue and green spectral regions (410–530 nm), where typical metal chalcogenide-based quantum dots suffer from photodegradation.

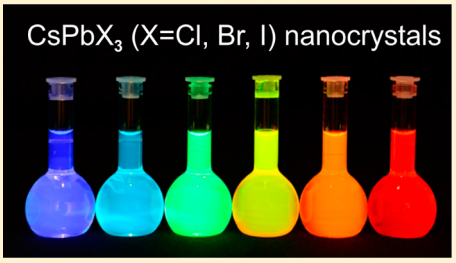

KEYWORDS: *Perovskites, halides, quantum dots, nanocrystals, optoelectronics*

Colloidal semiconductor nanocrystals (NCs, typically 2–20 nm large), also known as nanocrystal quantum dots (QDs), are being studied intensively as future optoelectronic materials.[1−4] These QD materials feature a very favorable combination of quantum-size effects, enhancing their optical properties with respect to their bulk counterparts, versatile surface chemistry, and a "free" colloidal state, allowing their dispersion into a variety of solvents and matrices and eventual incorporation into various devices. To date, the best developed optoelectronic NCs in terms of size, shape, and composition are binary and multinary (ternary, quaternary) metal chalcogenide NCs.[1,5−9] In contrast, the potential of semiconducting metal halides in the form of colloidal NCs remains rather unexplored. In this regard, recent reports on highly efficient photovoltaic devices with certified power conversion efficiencies approaching 20% using hybrid organic–inorganic lead halides $MAPbX_3$ (MA = CH_3NH_3, X = Cl, Br, and I) as semiconducting absorber layers are highly encouraging.[10−14]

In this study, we turn readers' attention to a closely related family of materials: all-inorganic cesium lead halide perovskites ($CsPbX_3$, X = Cl, Br, I, and mixed Cl/Br and Br/I systems; isostructural to perovskite $CaTiO_3$ and related oxides). These ternary compounds are far less soluble in common solvents (contrary to $MAPbX_3$), which is a shortcoming for direct solution processing but a necessary attribute for obtaining these compounds in the form of colloidal NCs. Although the synthesis, crystallography, and photoconductivity of direct bandgap $CsPbX_3$ have been reported more than 50 years ago,[15] they have never been explored in the form of colloidal nanomaterials.

Here we report a facile colloidal synthesis of monodisperse, 4–15 nm $CsPbX_3$ NCs with cubic shape and cubic perovskite crystal structure. $CsPbX_3$ NCs exhibit not only compositional bandgap engineering, but owing to the exciton Bohr diameter of up to 12 nm, also exhibit size-tunability of their bandgap energies through the entire visible spectral region of 410–700 nm. Photoluminescence (PL) of $CsPbX_3$ NCs is characterized by narrow emission line widths of 12–42 nm, high quantum yields of 50–90%, and short radiative lifetimes of 1–29 ns.

Received: December 19, 2014
Published: January 29, 2015

DOI: 10.1021/nl5048779
Nano Lett. 2015, 15, 3692–3696

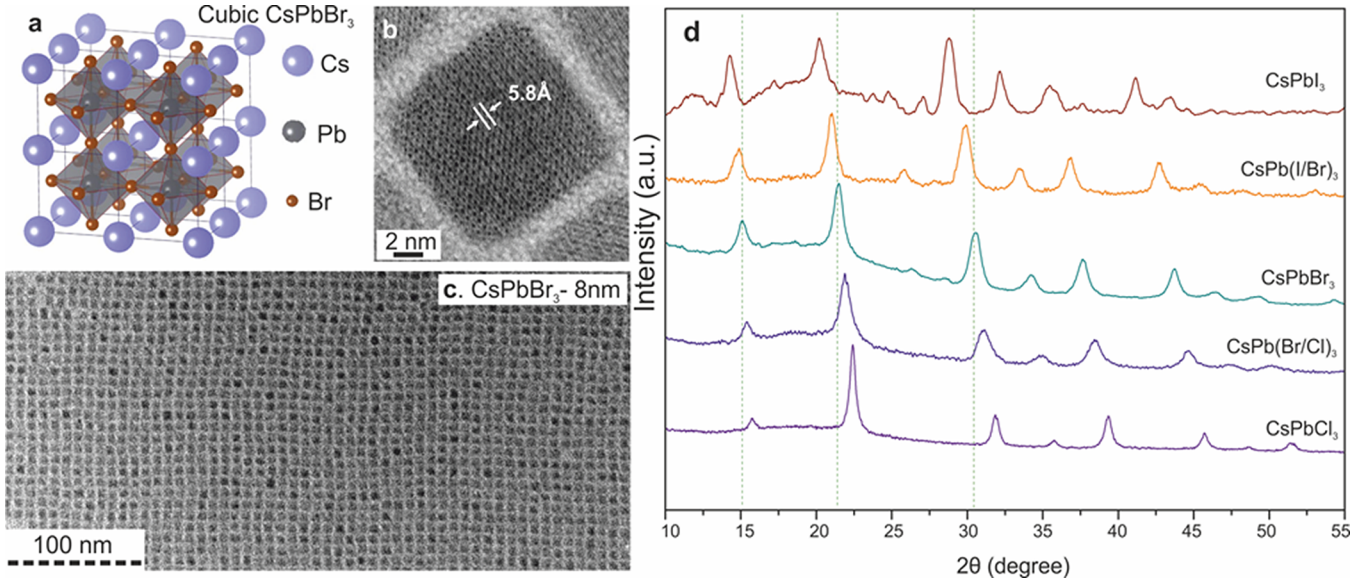

Figure 1. Monodisperse $CsPbX_3$ NCs and their structural characterization. (a) Schematic of the cubic perovskite lattice; (b,c) typical transmission electron microscopy (TEM) images of $CsPbBr_3$ NCs; (d) X-ray diffraction patterns for typical ternary and mixed-halide NCs.

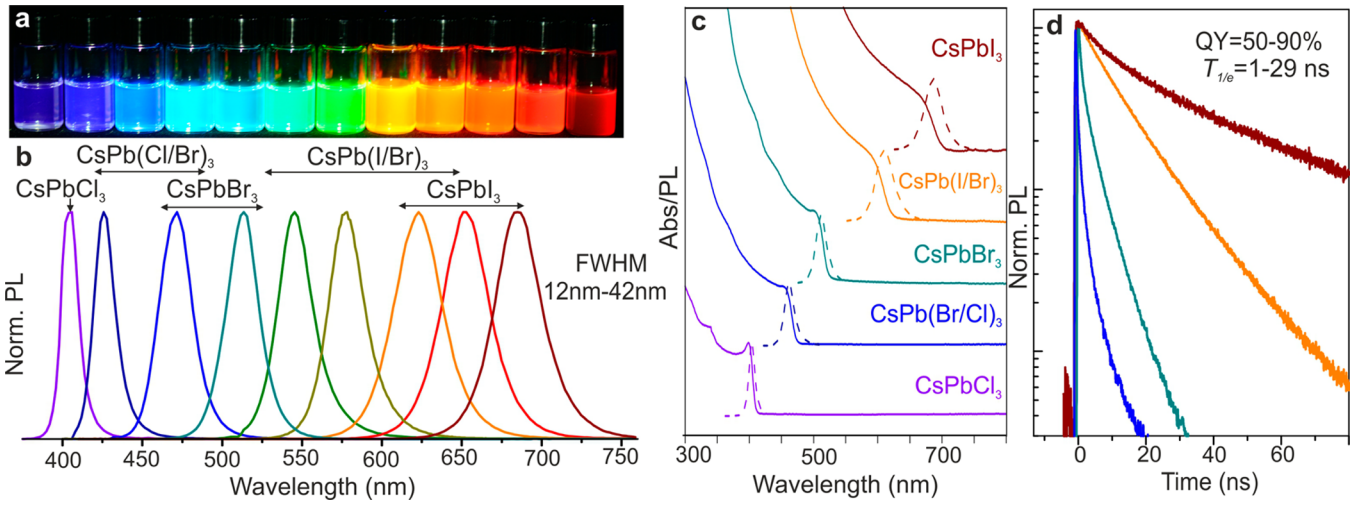

Figure 2. Colloidal perovskite $CsPbX_3$ NCs (X = Cl, Br, I) exhibit size- and composition-tunable bandgap energies covering the entire visible spectral region with narrow and bright emission: (a) colloidal solutions in toluene under UV lamp (λ = 365 nm); (b) representative PL spectra (λ_{exc} = 400 nm for all but 350 nm for $CsPbCl_3$ samples); (c) typical optical absorption and PL spectra; (d) time-resolved PL decays for all samples shown in (c) except $CsPbCl_3$.

Synthesis of Monodisperse $CsPbX_3$ NCs. Our solution-phase synthesis of monodisperse $CsPbX_3$ NCs (Figure 1) takes advantage of the ionic nature of the chemical bonding in these compounds. Controlled arrested precipitation of Cs^+, Pb^{2+}, and X^- ions into $CsPbX_3$ NCs is obtained by reacting Cs-oleate with a Pb(II)-halide in a high boiling solvent (octadecene) at 140−200 °C (for details, see the Supporting Information). A 1:1 mixture of oleylamine and oleic acid are added into octadecene to solubilize PbX_2 and to colloidally stabilize the NCs. As one would expect for an ionic metathesis reaction, the nucleation and growth kinetics are very fast. In situ PL measurements with a CCD-array detector (Supporting Information Figure S1) indicate that the majority of growth occurs within the first 1−3 s (faster for heavier halides). Consequently, the size of $CsPbX_3$ NCs can be most conveniently tuned in the range of 4−15 nm by the reaction temperature (140−200 °C) rather than by the growth time. Mixed-halide perovskites, that is, $CsPb(Cl/Br)_3$ and $CsPb(Br/I)_3$, can be readily produced by combining appropriate ratios of PbX_2 salts. Note that Cl/I perovskites cannot be obtained due to the large difference in ionic radii, which is in good agreement with the phase diagram for bulk materials.[16] Elemental analyses by energy dispersive X-ray (EDX) spectroscopy and by Ratherford backscattering spectrometry (RBS) confirmed the 1:1:3 atomic ratio for all samples of $CsPbX_3$ NCs, including mixed-halide systems.

$CsPbX_3$ are known to crystallize in orthorhombic, tetragonal, and cubic polymorphs of the perovskite lattice with the cubic phase being the high-temperature state for all compounds.[16−18] Interestingly, we find that all $CsPbX_3$ NCs crystallize in the cubic phase (Figure 1d), which can be attributed to the combined effect of the high synthesis temperature and contributions from the surface energy. For $CsPbI_3$ NCs, this is very much a metastable state, because bulk material converts

DOI: 10.1021/nl5048779
Nano Lett. 2015, 15, 3692−3696

into cubic polymorph only above 315 °C. At room temperature, an exclusively PL-inactive orthorhombic phase has been reported for bulk $CsPbI_3$ (a yellow phase).[16−19] Our first-principles total energy calculations (density functional theory, Figure S2, Table S1 in Supporting Information) confirm the bulk cubic $CsPbI_3$ phase to have 17 kJ/mol higher internal energy than the orthorhombic polymorph (7 kJ/mol difference for $CsPbBr_3$). Weak emission centered at ∼710 nm has been observed from melt-spun bulk $CsPbI_3$, shortly before recrystallization into the yellow phase.[18] Similarly, our solution synthesis of $CsPbI_3$ at 305 °C yields cubic-phase 100−200 nm NCs with weak, short-lived emission at 714 nm (1.74 eV), highlighting the importance of size reduction for stabilizing the cubic phase and indicating that all $CsPbI_3$ NCs in Figure 2b (5−15 nm in size) exhibit quantum-size effects (i.e., higher band gap energies due to quantum confinement, as discussed below). Cubic 4−15 nm $CsPbI_3$ NCs recrystallize into the yellow phase only upon extended storage (months), whereas all other compositions of $CsPbX_3$ NCs appear fully stable in a cubic phase.

Optical Properties of Colloidal $CsPbX_3$ NCs. Optical absorption and emission spectra of colloidal $CsPbX_3$ NCs (Figure 2b,c) can be tuned over the entire visible spectral region by adjusting their composition (ratio of halides in mixed halide NCs) and particle size (quantum-size effects). Remarkably bright PL of all NCs is characterized by high QY of 50−90% and narrow emission line widths of 12−42 nm. The combination of these two characteristics had been previously achieved only for core−shell chalcogenide-based QDs such as CdSe/CdS due to the narrow size distributions of the luminescent CdSe cores, combined with an epitaxially grown, electronically passivating CdS shell.[5,20] Time-resolved photoluminescence decays of $CsPbX_3$ NCs (Figure 2d) indicate radiative lifetimes in the range of 1−29 ns with faster emission for wider-gap NCs. For comparison, decay times of several 100 ns are typically observed in $MAPbI_3$ (PL peak at 765 nm, fwhm = 50 nm)[21] and 40−400 ns for $MAPbBr_{3-x}Cl_x$ (x = 0.6−2).[22]

Very bright emission of $CsPbX_3$ NCs indicates that contrary to uncoated chalcogenide NCs surface dangling bonds do not impart severe midgap trap states. This observation is also in good agreement with the high photophysical quality of hybrid organic−inorganic perovskites ($MAPbX_3$), despite their low-temperature solution-processing, which is generally considered to cause a high density of structural defects and trap states. In particular, thin-films of $MAPbX_3$ exhibit relatively high PL QYs of 20−40% at room temperature[23,24] and afford inexpensive photovoltaic devices approaching 20% in power conversion efficiency[10−12] and also electrically driven light-emitting devices.[25]

Ternary $CsPbX_3$ NCs compare favorably to common multinary chalcogenide NCs: both ternary ($CuInS_2$, $CuInSe_2$, $AgInS_2$, and $AgInSe_2$) and quaternary ($CuZnSnS_2$ and similar) compounds. $CsPbX_3$ materials are highly ionic and thus are rather stoichiometric and ordered due to the distinct size and charge of the Cs and Pb ions. This is different from multinary chalcogenide materials that exhibit significant disorder and inhomogeneity in the distribution of cations and anions owing to little difference between the different cationic and anionic sites (all are essentially tetrahedral). In addition, considerable stoichiometric deviations lead to a large density of donor−acceptor states due to various point defects (vacancies, interstitials, etc.) within the band gap, both shallow and deep. These effects eventually lead to absent or weak and broad emission spectra and long multiexponent lifetimes.[7,26−29]

For a colloidal semiconductor NC to exhibit quantum-dot-like properties (shown in Figures 2b and 3), the NC diameter

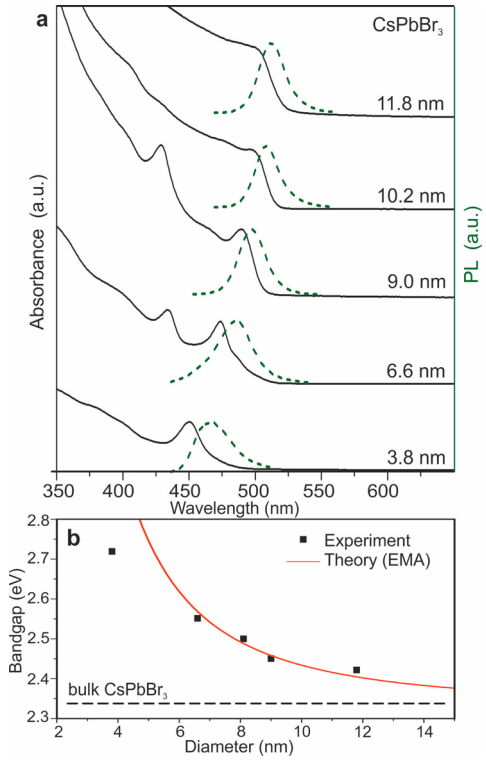

Figure 3. (a) Quantum-size effects in the absorption and emission spectra of 5−12 nm $CsPbBr_3$ NCs. (b) Experimental versus theoretical (effective mass approximation, EMA) size dependence of the band gap energy.

must be comparable or smaller than that of the natural delocalization lengths of an exciton in a bulk semiconductor (i.e., the exciton Bohr diameter, a_0). The electronic structure of $CsPbX_3$ (X = Cl, Br, and I), including scalar relativistic and spin−orbit interactions, was calculated using VASP code[30] and confirms that the upper valence band is formed predominately by the halide p-orbitals and the lower conduction band is formed by the overlap of the Pb p-orbitals (Figures S3 and S4 and Tables S2 and S3 in Supporting Information). Effective masses of the electrons and holes were estimated from the band dispersion, while the high-frequency dielectric constants were calculated by using density functional perturbation theory.[31] Within the effective mass approximation (EMA),[32] we have estimated the effective Bohr diameters of Wannier−Mott excitons and the binding energies for $CsPbCl_3$ (5 nm, 75 meV), $CsPbBr_3$ (7 nm, 40 meV), and $CsPbI_3$ (12 nm, 20 meV). Similarly, in closely related hybrid perovskite $MAPbI_3$ small exciton binding energies of ≤25 meV have been suggested computationally[33−35] and found experimentally.[36] For comparison, the typical exciton binding energies in organic semiconductors are above 100 meV. The confinement energy ($\Delta E = \hbar^2\pi^2/2m^*r^2$, where r is the particle radius and m^* is the reduced mass of the exciton) provides an estimate for the blue shift of the emission peak and absorption edge and is in good agreement with the experimental observations (Figure 3b).

Recently, highly luminescent semiconductor NCs based on Cd-chalcogenides have inspired innovative optoelectronic

DOI: 10.1021/nl5048779
Nano Lett. 2015, 15, 3692−3696

applications such as color-conversion LEDs, color-enhancers in backlight applications (e.g., Sony's 2013 Triluminos LCD displays), and solid-state lighting.[4,37,38] Compared to conventional rare-earth phosphors or organic polymers and dyes, NCs often show superior quantum efficiency and narrower PL spectra with fine-size tuning of the emission peaks and hence can produce saturated colors. A CIE chromaticity diagram (introduced by the Commision Internationale de l'Eclairage)[39] allows the comparison of the quality of colors by mapping colors visible to the human eye in terms of hue and saturation. For instance, well-optimized core−shell CdSe-based NCs cover ≥100% of the NTSC TV color standard (introduced in 1951 by the National Television System Committee).[39] Figure 4a shows that $CsPbX_3$ NCs allow a wide gamut of pure colors as well. Namely, a selected triangle of red, green, and blue emitting $CsPbX_3$ NCs encompasses 140% of the NTSC standard, extending mainly into red and green regions.

Light-emission applications, discussed above, and also luminescent solar concentrators[40,41] require solution-processability and miscibility of NC-emitters with organic and inorganic matrix materials. To demonstrate such robustness for $CsPbX_3$ NCs, we embedded them into poly(methylmetacrylate) (PMMA), yielding composites of excellent optical clarity and with bright emission (Figure 4b). To accomplish this, $CsPbX_3$ NCs were first dispersed in a liquid monomer (methylmetacrylate, MMA) as a solvent. Besides using known heat-induced polymerization with radical initiators,[41] we also performed polymerization already at room-temperature by adding a photoinitiator Irgacure 819 (bis(2,4,6-trimethylbenzoyl)-phenylphosphineoxide),[42] followed by 1h of UV-curing. We find that the presence of $CsPbX_3$ NCs increases the rate of photopolymerization, compared to a control experiment with pure MMA. This can be explained by the fact that the luminescence from $CsPbX_3$ NCs may be reabsorbed by the photoinitiator that has a strong absorption band in the visible spectral region, increasing the rate of polymerization.

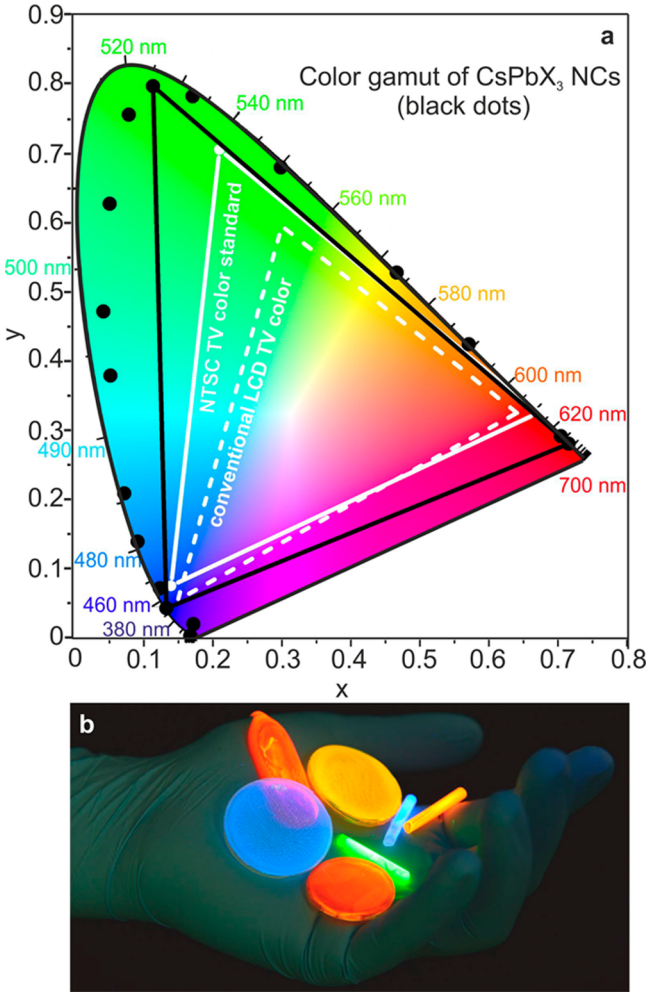

Figure 4. (a) Emission from $CsPbX_3$ NCs (black data points) plotted on CEI chromaticity coordinates and compared to most common color standards (LCD TV, dashed white triangle, and NTSC TV, solid white triangle). Radiant Imaging Color Calculator software from Radiant Zemax (http://www.radiantzemax.com) was used to map the colors. (b) Photograph (λ_{exc} = 365 nm) of highly luminescent $CsPbX_3$ NCs-PMMA polymer monoliths obtained with Irgacure 819 as photoinitiator for polymerization.

Conclusions. In summary, we have presented highly luminescent colloidal $CsPbX_3$ NCs (X = Cl, Br, I, and mixed Cl/Br and Br/I systems) with bright (QY = 50−90%), stable, spectrally narrow, and broadly tunable photoluminescence. Particularly appealing are highly stable blue and green emitting $CsPbX_3$ NCs (410−530 nm), because the corresponding metal-chalcogenide QDs show reduced chemical and photostability at these wavelengths. In our ongoing experiments, we find that this simple synthesis methodology is also applicable to other metal halides with related crystal structures (e.g., $CsGeI_3$, $Cs_3Bi_2I_9$, and Cs_2SnI_6, to be published elsewhere). Future studies with these novel QD-materials will concentrate on optoelectronic applications such as lasing, light-emitting diodes, photovoltaics, and photon detection.

■ ASSOCIATED CONTENT

Supporting Information

Synthesis details, calculations, and additional figures. This material is available free of charge via the Internet at http://pubs.acs.org.

■ AUTHOR INFORMATION

Corresponding Author

*E-mail: mvkovalenko@ethz.ch.

Author Contributions

The manuscript was prepared through the contribution of all coauthors. All authors have given approval to the final version of the manuscript.

Notes

The authors declare no competing financial interest.

■ ACKNOWLEDGMENTS

This work was financially supported by the European Research Council (ERC) via Starting Grant (306733). The work at Bath was supported by the ERC Starting Grant (277757) and by the EPSRC (Grants EP/M009580/1 and EP/K016288/1). Calculations at Bath were performed on ARCHER via the U.K.'s HPC Materials Chemistry Consortium (Grant EP/L000202). Calculations at ETH Zürich were performed on the central HPC cluster BRUTUS. We thank Nadia Schwitz for a help with photography, Professor Dr. H. Grützmacher and Dr. G. Müller for a sample of Irgacure 819 photoinitiator, Dr. F. Krumeich for EDX measurements, Dr. M. Döbeli for RBS measurements (ETH Laboratory of Ion Beam Physics), and Dr. N. Stadie for

DOI: 10.1021/nl5048779
Nano Lett. 2015, 15, 3692−3696

reading the manuscript. We gratefully acknowledge the support of the Electron Microscopy Center at Empa and the Scientific Center for Optical and Electron Microscopy (ScopeM) at ETH Zürich.

REFERENCES

(1) Talapin, D. V.; Lee, J.-S.; Kovalenko, M. V.; Shevchenko, E. V. *Chem. Rev.* **2009**, *110*, 389−458.
(2) Lan, X.; Masala, S.; Sargent, E. H. *Nat. Mater.* **2014**, *13*, 233−240.
(3) Hetsch, F.; Zhao, N.; Kershaw, S. V.; Rogach, A. L. *Mater. Today* **2013**, *16*, 312−325.
(4) Shirasaki, Y.; Supran, G. J.; Bawendi, M. G.; Bulovic, V. *Nat. Photonics* **2013**, *7*, 13−23.
(5) Chen, O.; Zhao, J.; Chauhan, V. P.; Cui, J.; Wong, C.; Harris, D. K.; Wei, H.; Han, H.-S.; Fukumura, D.; Jain, R. K.; Bawendi, M. G. *Nat. Mater.* **2013**, *12*, 445−451.
(6) Murray, C. B.; Norris, D. J.; Bawendi, M. G. *J. Am. Chem. Soc.* **1993**, *115*, 8706−8715.
(7) Aldakov, D.; Lefrancois, A.; Reiss, P. *J. Mater. Chem. C* **2013**, *1*, 3756−3776.
(8) Fan, F.-J.; Wu, L.; Yu, S.-H. *Energy Environ. Sci.* **2014**, *7*, 190−208.
(9) Yu, X.; Shavel, A.; An, X.; Luo, Z.; Ibáñez, M.; Cabot, A. *J. Am. Chem. Soc.* **2014**, *136*, 9236−9239.
(10) Gratzel, M. *Nat. Mater.* **2014**, *13*, 838−842.
(11) Green, M. A.; Ho-Baillie, A.; Snaith, H. J. *Nat. Photonics* **2014**, *8*, 506−514.
(12) Park, N.-G. *J. Phys. Chem. Lett.* **2013**, *4*, 2423−2429.
(13) Zhou, H.; Chen, Q.; Li, G.; Luo, S.; Song, T.-b.; Duan, H.-S.; Hong, Z.; You, J.; Liu, Y.; Yang, Y. *Science* **2014**, *345*, 542−546.
(14) Chung, I.; Lee, B.; He, J.; Chang, R. P. H.; Kanatzidis, M. G. *Nature* **2012**, *485*, 486−489.
(15) Moller, C. K. *Nature* **1958**, *182*, 1436−1436.
(16) Sharma, S.; Weiden, N.; Weiss, A. *Z. Phys. Chem.* **1992**, *175*, 63−80.
(17) Trots, D. M.; Myagkota, S. V. *J. Phys. Chem. Solids* **2008**, *69*, 2520−2526.
(18) Stoumpos, C. C.; Malliakas, C. D.; Kanatzidis, M. G. *Inorg. Chem.* **2013**, *52*, 9019−9038.
(19) Babin, V.; Fabeni, P.; Nikl, M.; Nitsch, K.; Pazzi, G. P.; Zazubovich, S. *Phys. Status Solidi B* **2001**, *226*, 419−428.
(20) Christodoulou, S.; Vaccaro, G.; Pinchetti, V.; De Donato, F.; Grim, J. Q.; Casu, A.; Genovese, A.; Vicidomini, G.; Diaspro, A.; Brovelli, S.; Manna, L.; Moreels, I. *J. Mater. Chem. C* **2014**, *2*, 3439−3447.
(21) Wehrenfennig, C.; Liu, M.; Snaith, H. J.; Johnston, M. B.; Herz, L. M. *J. Phys. Chem. Lett.* **2014**, *5*, 1300−1306.
(22) Zhang, M.; Yu, H.; Lyu, M.; Wang, Q.; Yun, J.-H.; Wang, L. *Chem. Commun.* **2014**, *50*, 11727−11730.
(23) Xing, G.; Mathews, N.; Lim, S. S.; Yantara, N.; Liu, X.; Sabba, D.; Grätzel, M.; Mhaisalkar, S.; Sum, T. C. *Nat. Mater.* **2014**, *13*, 476−480.
(24) Deschler, F.; Price, M.; Pathak, S.; Klintberg, L. E.; Jarausch, D.-D.; Higler, R.; Hüttner, S.; Leijtens, T.; Stranks, S. D.; Snaith, H. J.; Atatüre, M.; Phillips, R. T.; Friend, R. H. *J. Phys. Chem. Lett.* **2014**, *5*, 1421−1426.
(25) Tan, Z.-K.; Moghaddam, R. S.; Lai, M. L.; Docampo, P.; Higler, R.; Deschler, F.; Price, M.; Sadhanala, A.; Pazos, L. M.; Credgington, D.; Hanusch, F.; Bein, T.; Snaith, H. J.; Friend, R. H. *Nat. Nanotechnol.* **2014**, *9*, 687−692.
(26) Ueng, H. Y.; Hwang, H. L. *J. Phys. Chem. Solids* **1989**, *50*, 1297−1305.
(27) Huang, L.; Zhu, X.; Publicover, N. G.; Hunter, K. W.; Ahmadiantehrani, M.; de Bettencourt-Dias, A.; Bell, T. W. *J. Nanopart. Res.* **2013**, *15*, 2056.
(28) De Trizio, L.; Prato, M.; Genovese, A.; Casu, A.; Povia, M.; Simonutti, R.; Alcocer, M. J. P.; D'Andrea, C.; Tassone, F.; Manna, L. *Chem. Mater.* **2012**, *24*, 2400−2406.
(29) Zhang, W.; Zhong, X. *Inorg. Chem.* **2011**, *50*, 4065−4072.
(30) Kresse, G.; Joubert, D. *Phys. Rev. B* **1999**, *59*, 1758.
(31) Baroni, S.; de Gironcoli, S.; Dal Corso, A.; Giannozzi, P. *Rev. Mod. Phys.* **2001**, *73*, 515.
(32) Yu, P. Y.; Cardona, M. *Fundamentals of Semiconductors*; Springer: New York, 1996.
(33) Even, J.; Pedesseau, L.; Katan, C. *J. Phys. Chem. C* **2014**, *118*, 11566−11572.
(34) Frost, J. M.; Butler, K. T.; Brivio, F.; Hendon, C. H.; van Schilfgaarde, M.; Walsh, A. *Nano Lett.* **2014**, *14*, 2584−2590.
(35) Menéndez-Proupin, E.; Palacios, P.; Wahnón, P.; Conesa, J. *Phys. Rev. B* **2014**, *90*, 045207.
(36) Saba, M.; Cadelano, M.; Marongiu, D.; Chen, F.; Sarritzu, V.; Sestu, N.; Figus, C.; Aresti, M.; Piras, R.; Geddo Lehmann, A.; Cannas, C.; Musinu, A.; Quochi, F.; Mura, A.; Bongiovanni, G. *Nat. Commun.* **2014**, *5*, 5049.
(37) Kim, T.-H.; Jun, S.; Cho, K.-S.; Choi, B. L.; Jang, E. *MRS Bull.* **2013**, *38*, 712−720.
(38) Supran, G. J.; Shirasaki, Y.; Song, K. W.; Caruge, J.-M.; Kazlas, P. T.; Coe-Sullivan, S.; Andrew, T. L.; Bawendi, M. G.; Bulović, V. *MRS Bull.* **2013**, *38*, 703−711.
(39) Ye, S.; Xiao, F.; Pan, Y. X.; Ma, Y. Y.; Zhang, Q. Y. *Mater. Sci. Eng. R* **2010**, *71*, 1−34.
(40) Bomm, J.; Buechtemann, A.; Chatten, A. J.; Bose, R.; Farrell, D. J.; Chan, N. L. A.; Xiao, Y.; Slooff, L. H.; Meyer, T.; Meyer, A.; van Sark, W. G. J. H. M.; Koole, R. *Sol. Energy Mater. Sol. Cells* **2011**, *95*, 2087−2094.
(41) Meinardi, F.; Colombo, A.; Velizhanin, K. A.; Simonutti, R.; Lorenzon, M.; Beverina, L.; Viswanatha, R.; Klimov, V. I.; Brovelli, S. *Nat. Photonics* **2014**, *8*, 392−399.
(42) Gruetzmacher, H.; Geier, J.; Stein, D.; Ott, T.; Schoenberg, H.; Sommerlade, R. H.; Boulmaaz, S.; Wolf, J.-P.; Murer, P.; Ulrich, T. *Chimia* **2008**, *62*, 18−22.

NOTE ADDED AFTER ASAP PUBLICATION

This paper was published on the Web on February 2, 2015. The discussion of the preparation of Cs-oleate and synthesis of $CsPbX_3$ NCs in the Supporting Information has been corrected, and the paper was reposted on April 14, 2015.

DOI: 10.1021/nl5048779
Nano Lett. 2015, 15, 3692−3696